




# Comb-locked cavity ring-down spectroscopy with variable temperature

H. WU,<sup>1</sup> N. STOLARCZYK,<sup>1,2</sup> Q.-H. LIU,<sup>1</sup> C.-F. CHENG,<sup>1,3,\*</sup>  T.-P. HUA,<sup>1</sup> Y. R. SUN,<sup>1,3</sup>  AND S.-M. HU<sup>1,3</sup> 

<sup>1</sup>Hefei National Laboratory for Physical Sciences at Microscale, iChem center, University of Science and Technology of China, Hefei 230026, China

<sup>2</sup>Institute of Physics, Faculty of Physics, Astronomy and Informatics, Nicolaus Copernicus University in Torun, Grudziadzka 5, Torun 87-100, Poland

<sup>3</sup>CAS Center for Excellence in Quantum Information and Quantum Physics, University of Science and Technology of China, Hefei 230026, China

\*cfcheng@ustc.edu.cn

**Abstract:** Temperature dependence of molecular absorption line shape is important information for spectroscopic studies and applications. In this work, we report a comb-locked cavity ring-down spectrometer employing a cryogenic cooler to perform absorption spectroscopy measurements at temperatures between 40 K and 300 K. As a demonstration, we recorded the spectrum of the R(0) line in the (2-0) band of HD at 46 K. The temperature was also confirmed by the Doppler width of the HD line. Spectra of CH<sub>4</sub> near 1.394  $\mu\text{m}$  were also recorded in a wide temperature range of 70–300 K. Lower-state energies of methane lines were analyzed by fitting these spectra, which can be directly compared with the HITRAN and *TheoReTS* databases. Considerable deviations were observed, indicating the need to investigate the assignments of the methane lines in this region.

© 2019 Optical Society of America under the terms of the [OSA Open Access Publishing Agreement](#)

## 1. Introduction

Over the past two decades, molecular spectroscopy has owed its significant development to the cavity ring-down spectroscopy (CRDS) technique. Due to its remarkable sensitivity, a large amount of high-resolution spectral data have been acquired by CRDS [1–5]. However, spectra of some molecules are extremely dense at room temperature, which hinders the analysis and assignments of the transitions. A well-known example is the methane molecule, which is of great interest in the study of atmospheres of the Earth and other planets. Proper assignment of overlapping lines of methane has been a long-standing challenge in molecular spectroscopy.

Since the intensity of an absorption line depends on the number of molecules populating in the lower state, the change in temperature will lead to a remarkable change in the line intensity. Because the temperature dependence relies on the energy of the lower state of the transition, one can verify the assignment by observing the change of line intensities with temperatures. Besides, the spectral congestion is reduced when the temperature decreases, which is also beneficial for distinguishing adjacent spectral lines more efficiently.

Numerous spectrometers have been built to collect absorption spectra data at low temperatures [6–14], including those using supersonic expansion [15–18]. Some low-temperature absorption spectroscopy measurements utilize cavity ring-down spectroscopy techniques, e.g. phase-shift CRDS [19–22] and supersonic jet expansion CRDS [23,24]. Hodges' group developed a frequency-stabilized (FS)-CRDS setup for remote sensing applications of CO<sub>2</sub> and recorded the spectra in the temperature range of 220–290 K [25]. Development of the spectrometer operating at lower and wider temperature range has been motivated by various applications such as precision spectroscopy of the hydrogen molecule [26], analysis of methane spectrum in the near-IR range [27,28], and line-shape studies of molecules at low temperatures [29]. It is worth

noting that the capability to conduct measurements below the liquid-nitrogen temperature is useful for these studies, as the triple-point temperatures of the hydrogen and methane molecules are 13.8 K and 90.7 K, respectively. At lower temperatures, molecules exhibit narrower line widths and lower line densities, which effectively help to better resolve the line profiles.

Here we present a comb-locked cavity ring-down spectrometer with temperature variable in the range of 40–300 K. This apparatus allows us to investigate the temperature dependence of line shape, with spectral precision (x-axis) and signal-to-noise ratio (y-axis) commensurate with previous room-temperature CRDS instruments [30]. As a demonstration, spectra of HD and methane at 1.4  $\mu\text{m}$  were recorded at low temperatures. With this instrument, we expect to measure transitions of molecules in a large temperature range, resulting in more accurate spectroscopic data for precision measurements and line profile analysis.

## 2. Experimental setup

The experimental setup, shown in Fig. 1, is consisted of a high-sensitivity CRDS spectrometer integrated with a low-temperature gas cell. The optical configuration, shown in Fig. 1(a) is similar to the one presented in our previous studies [3,31]. A continuous-wave (CW) tunable external cavity diode laser (ECDL) was coupled to a 62-cm-long resonance cavity equipped with two high-reflectivity (HR) mirrors. The HR mirrors have a reflectivity of 99.998% and one of them was mounted on a piezoelectric actuator (PZT). The laser was locked to the ring-down cavity by

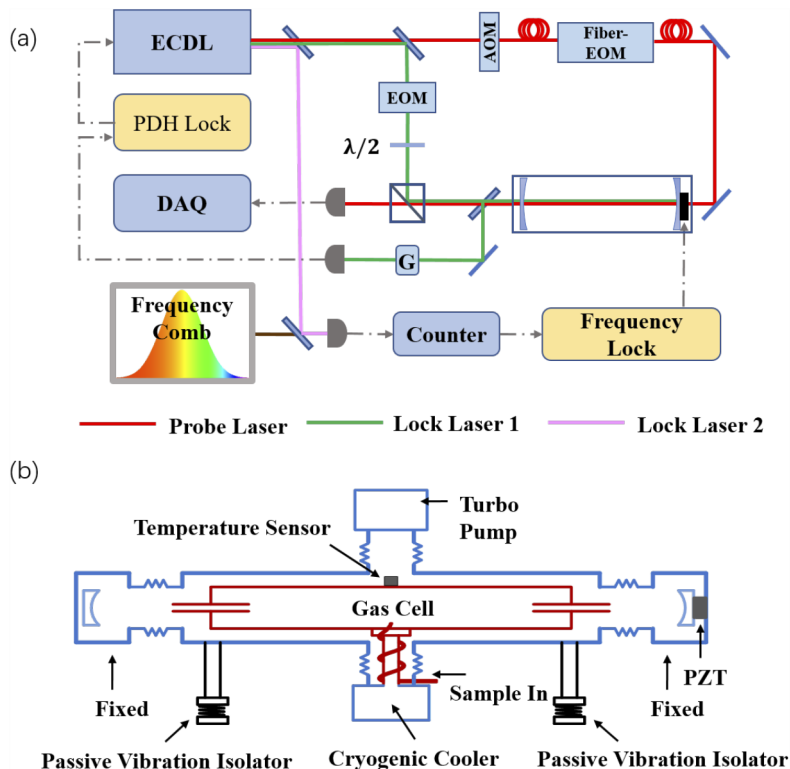


**Fig. 1.** (a) Scheme of the experimental setup. (b) Configuration of the optical cavity and vacuum chamber. Abbreviations: ECDL: external cavity diode laser; PDH Lock: Pound-Drever-Hall Lock; AOM: acousto-optic modulator; EOM: electro-optic modulator;  $\lambda/2$ : half waveplate; G: Glan-Taylor prism; DAQ: data acquisition system for CRDS signals; PZT: piezoelectric actuator.

the Pound-Drever-Hall (PDH) technique and its frequency was determined from the beat with an optical frequency comb (OFC). The repetition frequency and carrier offset frequency of the OFC were locked to radio-frequency sources referenced to a GPS-disciplined rubidium clock. The beat frequency was stabilized by a phase-locking servo controlling the PZT and consequently stabilizing the cavity length. The laser beam probing the ring-down signal was chopped by an acousto-optic modulator (AOM) and the light transmitted through the cavity was recorded and digitized. The signal of a ring-down event was fitted by an exponential decay function to derive the ring-down time,  $\tau$ . Subsequently, a fiber electro-optic modulator (EOM) produced a sideband used to scan the frequency of the probing laser beam. When the laser is locked to the cavity, one can perform a coarse spectral scan by tuning the EOM sideband frequency in a step equal to the free spectral range (FSR) of the cavity, while a fine scan can be realized by tuning the beat frequency between the laser and the OFC by controlling the PZT attached to the HR mirror.

Figure 1(b) shows the gas cell attached to the cryogenic cooler (Sumitomo RDK-205D). The cell was made of copper, wound with a heating wire (not shown in the figure), and the temperature was controlled in the range of 40-300 K with a stability of 1 K. To insulate the optical cavity from the vibrations generated by the cooler and the pumps, we have undertaken the following: (i) physically isolating the ring-down cavity mirrors with bellows, (ii) implementing passive vibration damping to hold the main vacuum chamber, (iii) isolating the turbo pump from the main chamber with bellows. To avoid the deposition of the sample on the HR mirrors at low temperature and a consequent drop of reflectivity, we used an open gas cell. The HR mirrors were separated from the cold gas cell and maintained at room temperature, which also isolated the mirrors from vibrations from the cryogenic compressor. Sample gas flowed continuously into the cold gas cell through a 3-mm-diameter pipe anchored to the cold finger of the cryogenic cooler. After the gas entered the cold cell, it flowed out along the pipeline into the outer chamber and was pumped away by the vacuum pump (or recycled back to the sample source chamber). The flow conductivity of the cavity was designed to keep the gas pressure inside the cold cell at the level of approximately 60 times that in the vacuum chamber outside the cell. A mass flowmeter was used to control the gas flow and stabilize the sample pressure. There is a region

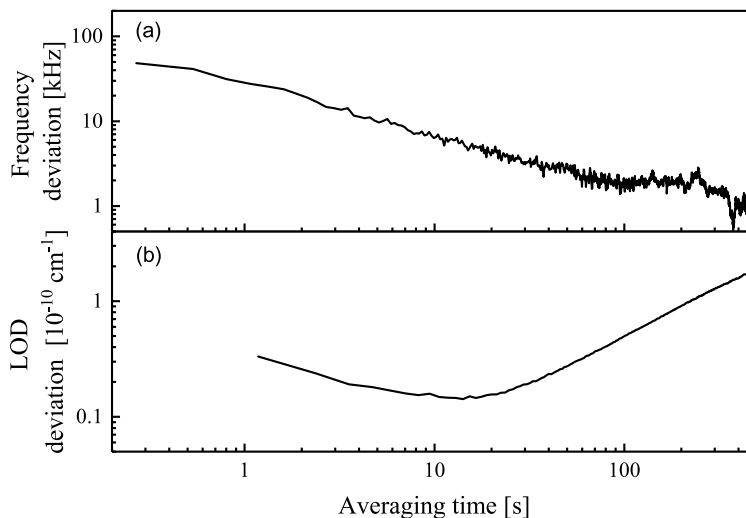


**Fig. 2.** Allan deviations of (a) The beat frequency between the laser and the OFC. (b) Limit of detection (in noise-equivalent absorption coefficient) of the CRDS spectrometer. The data were collected at the gas cell temperature of 46 K when the cryogenic cooler and vacuum pumps were on. The repetition rate of the ring-down events was 1 kHz.

between each HR mirror and the end face of the cold cell in which the gas temperature increased gradually to room temperature. However, the length of this region only accounts for less than 15% of the length of the entire optical cavity, and the gas pressure was close to the background of the vacuum chamber. Consequently, the contribution from the absorption of thermal molecules is negligible.

Figure 2(a) shows the Allan deviation of the beat frequency, indicating that the laser frequency followed well with the comb tooth, and the long-term drift was below 2 kHz in 100 seconds. Figure 2(b) depicts the Allan deviation of the absorption coefficient of the empty cavity. The limit of detection (LOD), in terms of the noise-equivalent absorption coefficient, reaches  $1.5 \times 10^{-11} \text{ cm}^{-1}$  at an averaging time of 10 s.

### 3. Results and discussion

To test the setup, we recorded the spectrum of the R(0) line in the (2-0) band of HD at around 46 K, where the temperature of the cold cell is directly read from the temperature sensor shown in Fig. 1(b). According to the HITRAN database, the R(0) (2-0) line is located at  $7168.470 \text{ cm}^{-1}$ , with an intensity of  $2.444 \times 10^{-25} \text{ cm}^{-1}/(\text{molecule cm}^{-2})$  [32]. Due to the mass difference between proton and deuteron, the HD molecule has a small permanent dipole moment, resulting in dipole transitions stronger than its quadrupole transitions. Despite the extremely weak transition strength, the main difficulty of the measurement came from the nearby strong water absorption lines. Optical elements outside the vacuum chamber were sealed in a plexiglass box filled with dry air to prevent the power loss of the laser beam due to the presence of water vapor in the optical path. The spectra were recorded at an HD sample pressure of about 0.6 Pa. The decrease of the temperature diminishes the vapor pressure of water in the gas cell (reducing contamination in the sample gas). The spectral scan was performed by making use of the EOM sideband. At each frequency point, around 1000 ring-down events were recorded within an acquisition time of about one second. Each scan took about 16 s with a typical frequency step of 240 MHz which equals to the FSR of the ring-down cavity. An averaged spectrum of 10 scans is presented in Fig. 3, which was fitted by a Gaussian profile. At such a low pressure, the collision-induced broadening and shift, and more sophisticated pressure-dependent effects [33] are negligible. The line width was derived from the fit, which gave a line width (full width at half maximum, FWHM) of  $611 \pm 16 \text{ MHz}$ , corresponding to the temperature of  $47.7 \pm 2.5 \text{ K}$ . The uncertainty is mainly from the fitting error and the result agrees well with the reading of the temperature sensor.

As a demonstration of the wide temperature operation range of the system, we recorded the absorption spectrum of methane at  $1.4 \mu\text{m}$ . The density of the methane lines is very high in this range. Since our goal was the observation of the temperature dependence of line intensities instead of precise line centers, the conventional CRDS method [30] was applied. We did not lock the laser to the cavity with the PDH method but used the dithering-PZT method to match the cavity mode with the laser frequency, which was monitored by a wavemeter. The PZT was scanned with a frequency of 40 Hz, and at each laser frequency about 100 ring-down events were recorded. This method allows us to perform a fast spectral scan over a range of about 10 GHz with a step of about 60 MHz and an accuracy better than 10 MHz. As depicted in Fig. 4, two pieces of spectrum were investigated, one in the range of  $7175.01\text{-}7175.2 \text{ cm}^{-1}$  and the other in the range of  $7173.38\text{-}7173.67 \text{ cm}^{-1}$  (referred to as the “first” range and the “second”, respectively). In each of the two spectral ranges, we performed a series of measurements at five different temperatures between 70 K and 300 K. The choice of the minimum temperature of 70 K was made to avoid condensation of methane in the gas cell.

Due to the open-cavity design of our sample cell, the pressure of the sample inside the gas cell can not be measured directly. We regulated it by controlling the flow rate through the flowmeter. In the data analysis, the gas sample pressure was derived from the observed absorbance of a selected line (“f” on Fig. 4) according to its line intensity given in HITRAN [32]. The sample

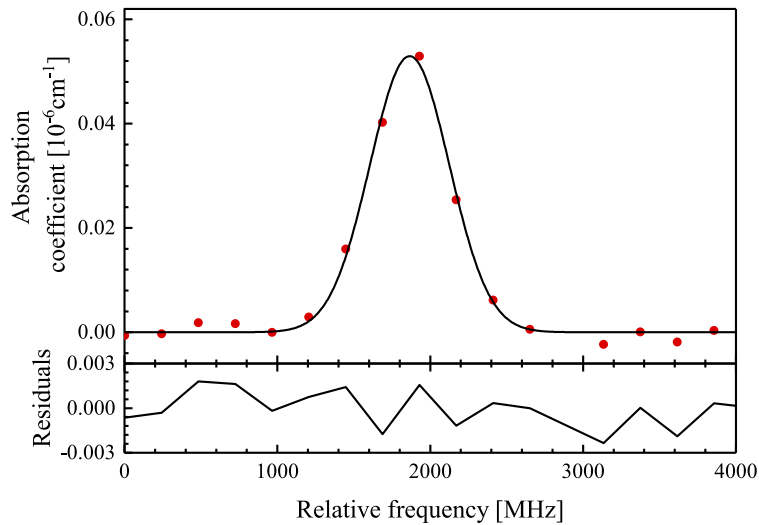


**Fig. 3.** Doppler broadened R(0) line in the (2-0) band of HD at 46 K.

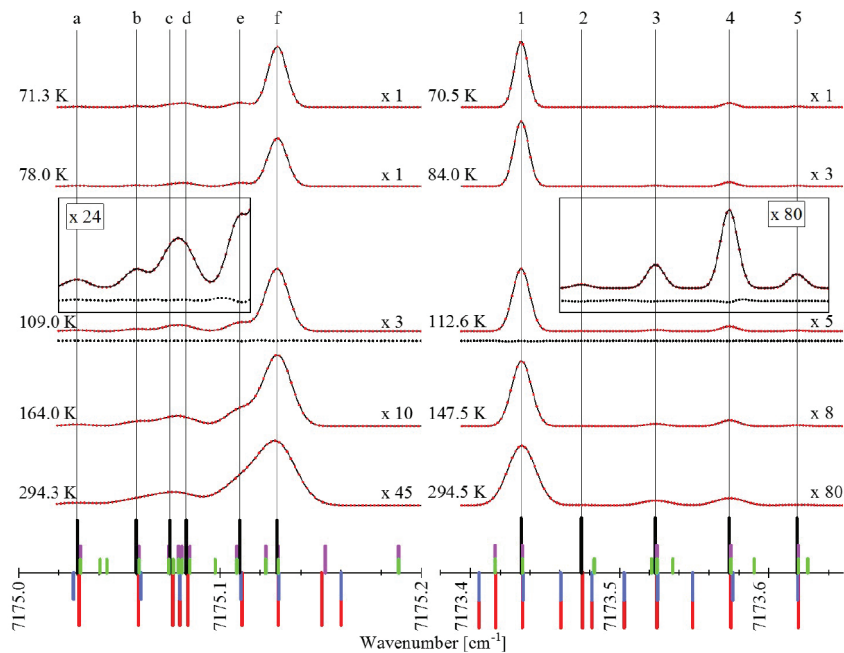


**Fig. 4.** Spectra of methane recorded at different temperatures. The upper part contains the experimental (red dots) and simulated (black lines) spectra. Annotations on the right side mark the magnification used to make the spectra visually comparable. Fitting residuals of the spectra recorded around 110 K are shown as black points beneath the spectra. In the lower part, colored bars indicate line positions obtained from different sources: this work (black bars), *TheoReTS* [34] (296 K, green bars and 80 K, purple bars), and WKL<sub>MC</sub> [28] (80 K, red bars and 296 K, blue bars). Note that the cut-off intensity of  $1 \times 10^{-25}$  cm/molecule was applied to the data from *TheoReTS* [34].

pressure was estimated to be about 0.1 Pa in our measurements, and each of the spectra presented in Fig. 4 was rescaled to the same sample pressure of 0.1 Pa. Note that the validity of the aforementioned calibration procedure relies on the correctness of the parameters of the reference line, but it does not change relative line intensities which could be derived directly from the observed spectra. A global multi-peak fitting procedure was applied to fit the spectra shown in Fig. 4. Since the spectra were recorded at very low pressures of about 0.1 Pa, simple Gaussian line profiles were applied in the fit, and adjustable parameters were the line positions and intensities, as well as a linear baseline. We found that at least six and five lines were needed in the fit of the spectra in the first and second ranges, respectively. Typical fitting residuals are below 1 % of the amplitude of the corresponding peak, which are illustrated in Fig. 4.

According to the HITRAN database [32], seven methane lines are located in the first spectral range and eleven in the second range. Here the HITRAN database uses the data from [28] (named WKLMC line list), where the line parameters were derived from the spectra recorded at 80 K and 296 K, shown as red and blue bars in Fig. 4, respectively. From the spectra obtained in this work, we were able to distinguish six and five lines in the first and second ranges, respectively, and their positions are marked as lines “a-f” and “1-5” in Fig. 4. These 11 lines coincide with the most intense ones given by the HITRAN database [32]. We found that two overlapped lines at  $7175.08 \text{ cm}^{-1}$  (marked as “c” and “d” in Fig. 4) were given as a single line by HITRAN. However, the observed spectra cannot be fitted well with a single line but could be fit with two lines (see fitting residuals shown in the inset of Fig. 4), indicating that the peak consists of at least two lines. As a comparison, the *TheoReTS* [34] database (green bars in Fig. 4) lists four lines at  $7175.08 \text{ cm}^{-1}$ . In the second range, many more lines were reported in WKLMC [28] than those given in this work, probably because in our experiment the sample pressure was much smaller.

Using relative line intensities of the transitions obtained from the fit, we derived the differences between the lower-state energies of the transitions [35],

$$\begin{aligned} \frac{S_i}{S_j} &= K_a \exp\left(\frac{hc(E_j'' - E_i'')}{k_B T}\right), \\ \ln \frac{S_i}{S_j} &= \ln K_a + \frac{hc(E_j'' - E_i'')}{k_B} \frac{1}{T}, \end{aligned} \quad (1)$$

where  $S_i$  and  $S_j$  are intensities of transitions  $i$  and  $j$ , respectively.  $E_i''$  and  $E_j''$  are the corresponding lower-state energies.  $K_a$  is a constant scaling factor independent from the temperature.  $h$ ,  $c$  and  $k_B$  are the Planck constant, speed of light, and Boltzmann constant, respectively. Figure 5 depicts the inverse-temperature dependence of the logarithmic intensity ratio between a pair of lines.

According to Eq. 1, a linear fit yielded the difference between the lower-state energies of the two transitions. The results are presented in Table 1., juxtaposed with values from the *TheoReTS* database [34] and the WKLMC dataset [28]. As shown in Table 1., in most cases, our results agree with both reference datasets within three times of our confidence intervals. However, there are still a few outliers in the table. In the vicinity of lines, “c” and “d”, no lower-state energies are given in the HITRAN database [32]. WKLMC [28] lists three lines but only one of them has an assignment, while four lines with strengths larger than  $1 \times 10^{-25} \text{ cm/molecule}$  are given in the *TheoReTS* database [34]. Another example is the line “2”, which was detected in our measurement, but it was not observed at room temperature in the WKLMC line list [28]. The lower-state energy difference between lines “1” and “2” given by the *TheoReTS* database deviates significantly from that given in this work, indicating that either the assignments or the calculated intensities of these two lines were incorrect in *TheoReTS*.

Differences of the lower-state energies derived from relative line intensities obtained at different temperatures could be more reliable for checking the line assignments since they are independent to sample pressures. Our work reports the observation of the spectrum at more temperatures than



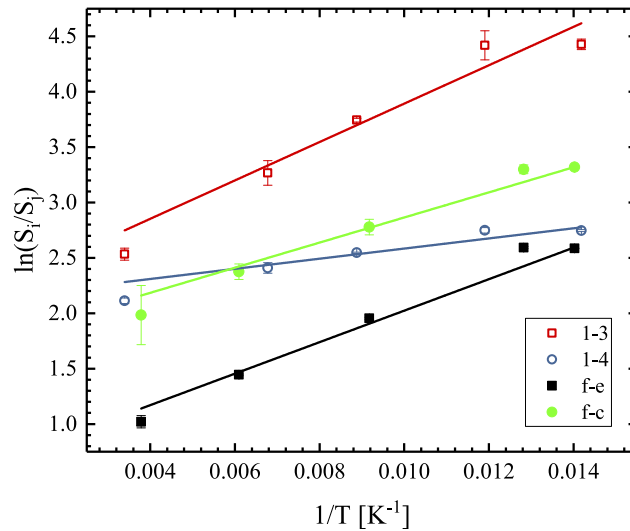


**Fig. 5.** A few examples of the relationship between the intensity ratio between a pair of lines and the inverse of the temperature.

**Table 1.** Lower state energy difference between the transitions (in  $\text{cm}^{-1}$ )<sup>a</sup>.

$i-j$	This work		WKLMLC	<i>TheoReTS</i>
	$E''_i - E''_j$	Uncertainty	$E''_i - E''_j$	$E''_i - E''_j$
a-f	90.4	10.4	118.35	73.3
b-f	117.7	3.5	133.44	125.7 <sup>b</sup>
c-f	78.5	12.9		
d-f	24.7	3.1		
e-f	98.6	9.4	120.04	125.7 <sup>b</sup>
2-1	38.9	2.5		470.8
3-1	120.5	24.2	166.46	157.1
4-1	31.8	8.4	63.84	31.4
5-1	30.7	13.2	66.52	62.9

<sup>a</sup>Data taken from [28] and [34] are marked with WKLMLC and *TheoReTS*, respectively. The uncertainties of the data from WKLMLC are not given in [28] but a typical uncertainty of  $0.25 \text{ cm}^{-1}$  was given in [36]. The uncertainties of the data from *TheoReTS* [34] were given as  $0.1-1 \text{ cm}^{-1}$ .

<sup>b</sup>*TheoReTS* proposed the same lower state energy for line b and e.

that in [28] where measurements were only performed at two temperatures of 80 K and 296 K. Although relatively small uncertainties ( $<1 \text{ cm}^{-1}$ ) for the lower state energies were given for moderate lines in WKLMLC [28,36] and *TheoReTS* [34], discrepancies were found by comparing the results obtained in this work. Our analysis gives the difference in lower-state energies of the lines “1” and “4” as  $31.8 \pm 8.4 \text{ cm}^{-1}$ , agreeing well with the value of  $31.4 \text{ cm}^{-1}$  given by the *TheoReTS* database [34], but deviating from that provided by WKLMLC [28]. It is also worth noting that the intensity of the line “1” given in HITRAN [32] agrees neither with our result nor with that from *TheoReTS* [34]. This discrepancy implies an incorrect assignment of line “1”, which may be overcome by further analysis using results obtained from our instrument.

#### 4. Conclusion

Summarizing, we report the construction of a cavity ring-down spectrometer integrated with an open sample cell which can operate in a temperature range of 40–300 K. We demonstrated the measurement of the R(0) line in the (2–0) band of HD at 1.395  $\mu\text{m}$  at a temperature of 46 K, free from the interference due to nearby strong water lines. We also recorded methane spectra near 1.394  $\mu\text{m}$  at temperatures between 70 and 295 K. In total 11 rovibrational transitions in the ranges of 7173.38–7173.67  $\text{cm}^{-1}$  and 7175.01–7175.2  $\text{cm}^{-1}$  were observed. Lower-state energies of these transitions were derived, according to the analysis of the temperature dependence of relative line intensities. The results were compared with the HITRAN and *TheoReTS* spectroscopic databases, showing disagreements for a few methane lines with previous studies. As demonstrated in this work, we believe the spectrometer could be useful in precision spectroscopy and many applications, including improving the accuracy of the spectroscopy of the hydrogen molecule, which is of great interest in fundamental physics, and quantitative analysis of the methane spectrum, which is of great need in studies of atmospheres of earth-like planets.

#### Funding

National Natural Science Foundation of China (21427804, 21688102, 11974328); Chinese Academy of Sciences (XDB21020100).

#### Acknowledgments

The authors acknowledge Y. Tan and A. -W. Liu from USTC for helpful discussion and suggestions.

#### Disclosures

The authors declare no conflicts of interest.

#### References

1. A. J. Fleisher, E. M. Adkins, Z. D. Reed, H. Yi, D. A. Long, H. M. Fleurbaey, and J. T. Hodges, “Twenty-five-fold reduction in measurement uncertainty for a molecular line intensity,” *Phys. Rev. Lett.* **123**(4), 043001 (2019).
2. O. L. Polyansky, K. Bielska, M. Ghysels, L. Lodi, N. F. Zobov, J. T. Hodges, and J. Tennyson, “High-accuracy CO<sub>2</sub> line intensities determined from theory and experiment,” *Phys. Rev. Lett.* **114**(24), 243001 (2015).
3. J. Wang, Y. R. Sun, L.-G. Tao, A.-W. Liu, and S.-M. Hu, “Communication: molecular near-infrared transitions determined with sub-kHz accuracy,” *J. Chem. Phys.* **147**(9), 091103 (2017).
4. Y. Tan, S. N. Mikhailenko, J. Wang, A.-W. Liu, X.-Q. Zhao, G.-L. Liu, and S.-M. Hu, “CRDS absorption spectrum of <sup>17</sup>O enriched water vapor in the 12,277–12,894  $\text{cm}^{-1}$  range,” *J. Quant. Spectrosc. Radiat. Transfer* **221**, 233–242 (2018).
5. O. Lyulin, S. Béguier, S.-M. Hu, and A. Campargue, “The absorption spectrum of acetylene near 1  $\mu\text{m}$  (9280–10740  $\text{cm}^{-1}$ ) (I): Line positions,” *J. Quant. Spectrosc. Radiat. Transfer* **208**, 179–187 (2018).
6. F. L. Hoch, “Low-temperature absorption spectroscopy (cryoabsorption spectroscopy),” *J. Chem. Educ.* **32**(9), 469–471 (1955).
7. D. R. Willey, R. L. Crownover, D. N. Bittner, and F. C. De Lucia, “Very low temperature spectroscopy: The pressure broadening coefficients for CO-He between 4.3 and 1.7 K,” *J. Chem. Phys.* **89**(4), 1923–1928 (1988).
8. G. J. SchererKevin, K. Lehmann, and W. Klemperer, “The high-resolution visible overtone spectrum of CH<sub>4</sub> and CD<sub>3</sub>H at 77 K,” *J. Chem. Phys.* **81**(12), 5319–5325 (1984).
9. J. J. O’Brien and H. Cao, “Absorption spectra and absorption coefficients for methane in the 750–940 nm region obtained by intracavity laser spectroscopy,” *J. Quant. Spectrosc. Radiat. Transfer* **75**(3), 323–350 (2002).
10. K. Singh and J. J. O’Brien, “Laboratory measurements of absorption coefficients for the 727 nm band of methane at 77 K and comparison with results derived from spectra of the Giant planets,” *J. Quant. Spectrosc. Radiat. Transfer* **54**(4), 607–619 (1995).
11. G. Pierre, J.-C. Hilico, C. de Bergh, and J.-P. Maillard, “The region of the 3 $\nu_3$  band of methane,” *J. Mol. Spectrosc.* **82**(2), 379–393 (1980).
12. T. Tsukamoto and H. Sasada, “Extended assignments of the 3 $\nu_1$  +  $\nu_3$  band of methane,” *J. Chem. Phys.* **102**(13), 5126–5140 (1995).
13. K. Boraas, D. Deboer, Z. Lin, and J. P. Reilly, “The Stark effect in methane’s 3 $\nu_1$  +  $\nu_3$  vibrational overtone band,” *J. Chem. Phys.* **99**(2), 1429–1432 (1993).



14. L. Yang, H. Lin, X. J. Feng, and J. T. Zhang, "Temperature-scanning saturation cavity ringdown spectrometry for Doppler-free spectroscopy," *Opt. Express* **26**(8), 10203–10210 (2018).
15. A. Campargue, M. Chenevier, and F. Stoeckel, "Intracavity-laser-absorption spectroscopy of the visible overtone transition of methane in a supersonically cooled jet," *Chem. Phys. Lett.* **183**(1-2), 153–157 (1991).
16. A. Campargue, D. Permogorov, and R. Jost, "Intracavity absorption spectroscopy of the third stretching overtone transition of jet cooled methane," *J. Chem. Phys.* **102**(15), 5910–5916 (1995).
17. A. Amrein, M. Quack, and U. Schmitt, "High-resolution interferometric Fourier transform infrared absorption spectroscopy in supersonic free jet expansions: carbon monoxide, nitric oxide, methane, ethyne, propyne, and trifluoromethane," *J. Phys. Chem.* **92**(19), 5455–5466 (1988).
18. K. Boraas, D. Deboer, Z. Lin, and J. P. Reilly, "High resolution study of methane's  $3\nu_1 + \nu_3$  vibrational overtone band," *J. Chem. Phys.* **100**(11), 7916–7927 (1994).
19. C. Moehnke, E. K. Lewis, A. Lopez-Calvo, and C. Manzanares, "Phase shift cavity ring down at low temperatures: Vibration-rotation overtone absorption of H-D ( $\Delta\nu = 4$ ) at 297 and 105 K," *Chem. Phys. Lett.* **418**(4-6), 576–580 (2006).
20. E. K. Lewis, C. Moehnke, J. Navea, and C. Manzanares, "Low temperature cell for cavity ring down absorption studies," *Rev. Sci. Instrum.* **77**(7), 073107 (2006).
21. Y. Perez-Delgado and C. Manzanares, "Cavity ring down and Fourier transform infrared spectroscopy at low temperatures (84-297 K): Fermi resonance and intensities of the C-H fundamental and overtone ( $\Delta\nu = 1-6$ ) transitions of CHD<sub>3</sub>," *J. Phys. Chem. A* **114**(30), 7918–7927 (2010).
22. Y. Perez-Delgado and C. Manzanares, "Low temperature cavity ring down spectroscopy with off-axis alignment: application to the A- and  $\gamma$ -bands of O<sub>2</sub> in the visible at 90 K," *Appl. Phys. B* **106**(4), 971–978 (2012).
23. M. Hippler and M. Quack, "Cw cavity ring-down infrared absorption spectroscopy in pulsed supersonic jets: nitrous oxide and methane," *Chem. Phys. Lett.* **314**(3-4), 273–281 (1999).
24. M. Hippler and M. Quack, "High-resolution Fourier transform infrared and cw-diode laser cavity ringdown spectroscopy of the  $\nu_2 + 2\nu_3$  band of methane near 7510 cm<sup>-1</sup> in slit jet expansions and at room temperature," *J. Chem. Phys.* **116**(14), 6045–6055 (2002).
25. M. Ghysels, Q. Liu, A. J. Fleisher, and J. T. Hodges, "A variable-temperature cavity ring-down spectrometer with application to line shape analysis of CO<sub>2</sub> spectra in the 1600 nm region," *Appl. Phys. B* **123**(4), 124 (2017).
26. L.-G. Tao, A.-W. Liu, K. Pachucki, J. Komasa, Y. R. Sun, J. Wang, and S.-M. Hu, "Toward a determination of the Proton-electron mass ratio from the Lamb-dip measurement of HD," *Phys. Rev. Lett.* **120**(15), 153001 (2018).
27. A. Campargue, O. Leshchishina, L. Wang, D. Mondelain, S. Kassı, and A. V. Nikitin, "Refinements of the WKMC empirical line lists (5852-7919 cm<sup>-1</sup>) for methane between 80 K and 296 K," *J. Quant. Spectrosc. Radiat. Transfer* **113**(15), 1855–1873 (2012).
28. A. Campargue, O. Leshchishina, L. Wang, D. Mondelain, and S. Kassı, "The WKLMC empirical line lists (5852–7919 cm<sup>-1</sup>) for methane between 80 K and 296 K: "final" lists for atmospheric and planetary applications," *J. Mol. Spectrosc.* **291**, 16–22 (2013).
29. D. ChrisBenner, V. MalathyDevi, K. Sung, L. R. Brown, C. E. Miller, V. H. Payne, B. J. Drouin, S. Yu, T. J. Crawford, A. W. Mantz, M. A. H. Smith, and R. R. Gamache, "Line parameters including temperature dependences of air- and self-broadened line shapes of <sup>12</sup>C<sup>16</sup>O<sub>2</sub>: 2.06- $\mu$ m region," *J. Mol. Spectrosc.* **326**, 21–47 (2016).
30. C.-F. Cheng, Y. R. Sun, H. Pan, Y. Lu, X.-F. Li, J. Wang, A.-W. Liu, and S.-M. Hu, "Cavity ring-down spectroscopy of Doppler-broadened absorption line with sub-MHz absolute frequency accuracy," *Opt. Express* **20**(9), 9956–9961 (2012).
31. L.-G. Tao, T.-P. Hua, Y. R. Sun, J. Wang, A.-W. Liu, and S.-M. Hu, "Frequency metrology of the acetylene lines near 789 nm from Lamb-dip measurements," *J. Quant. Spectrosc. Radiat. Transfer* **210**, 111–115 (2018).
32. I. E. Gordon, L. S. Rothman, C. Hill, R. V. Kochanov, Y. Tan, P. F. Bernath, M. Birk, V. Boudon, A. Campargue, K. V. Chance, B. J. Drouin, J. M. Flaud, R. R. Gamache, J. T. Hodges, D. Jacquemart, V. I. Perevalov, A. Perrin, K. P. Shine, M. A. H. Smith, J. Tennyson, G. C. Toon, H. Tran, V. G. Tyuterev, A. Barbe, A. G. Császár, V. M. Devi, T. Furtenbacher, J. J. Harrison, J. M. Hartmann, A. Jolly, T. J. Johnson, T. Karman, I. Kleiner, A. A. Kyuberis, J. Loos, O. M. Lyulin, S. T. Massie, S. N. Mikhailenko, N. Moazzen-Ahmadi, H. S. P. Müller, O. V. Naumenko, A. V. Nikitin, O. L. Polyansky, M. Rey, M. Rotger, S. W. Sharpe, K. Sung, E. Starikova, S. A. Tashkun, J. V. Auwera, G. Wagner, J. Wilzewski, P. Wcisło, S. Yu, and E. J. Zak, "The HITRAN2016 molecular spectroscopic database," *J. Quant. Spectrosc. Radiat. Transfer* **203**, 3–69 (2017).
33. N. H. Ngo, D. Lisak, H. Tran, and J. M. Hartmann, "An isolated line-shape model to go beyond the Voigt profile in spectroscopic databases and radiative transfer codes," *J. Quant. Spectrosc. Radiat. Transfer* **129**, 89–100 (2013).
34. M. Rey, A. V. Nikitin, Y. L. Babikov, and V. G. Tyuterev, "TheoReTS—An information system for theoretical spectra based on variational predictions from molecular potential energy and dipole moment surfaces," *J. Mol. Spectrosc.* **327**, 138–158 (2016).
35. M. Šimečková, D. Jacquemart, L. S. Rothman, R. R. Gamache, and A. Goldman, "Einstein A-coefficients and statistical weights for molecular absorption transitions in the HITRAN database," *J. Quant. Spectrosc. Radiat. Transfer* **98**(1), 130–155 (2006).
36. S. Kassı, B. Gao, D. Romania, and A. Campargue, "The near-infrared (1.30-1.70  $\mu$ m) absorption spectrum of methane down to 77 K," *Phys. Chem. Chem. Phys.* **10**(30), 4410–4419 (2008).